ROBUST CONTROL OF ROBOT MANIPULATORS USING FRACTIONAL ORDER LAG COMPENSATOR

Petar D. Mandić[1], Mihailo P. Lazarević[1], Tomislav B. Šekara[2], Marko Č. Bošković[3], Guido Maione[4]

[1]Faculty of Mechanical Engineering,
 University of Belgrade, Kraljice Marije 16, Belgrade, Serbia
 e-mail: pmandic@mas.bg.ac.rs, mlazarevic@mas.bg.ac.rs
[2]School of Electrical Engineering,
 University of Belgrade, Bulevar kralja Aleksandra 73, Belgrade, Serbia
 e-mail: tomi@etf.rs
[3]Faculty of Electrical Engineering,
 University of East Sarajevo, Vuka Karadžića 30, East Sarajevo, RS, Bosnia and Herzegovina
 e-mail: marko.boskovic@etf.ues.rs.ba
[4]Department of Electrical and Information Engineering,
 Polytechnic University of Bari, Via E. Orabona 4, Bari, Italy
 e-mail: guido.maione@poliba.it

Abstract:

In this paper a fractional order lag compensator is introduced for the control of robot manipulators. Mathematical model of the robotic system is derived using the Rodriquez approach which, due to a high gear ratio between the actuators and robot joints, reduces to a linear model. Then, fractional order compensator is designed according to the symmetrical optimum principle. Optimal values of controller parameters give good performance characteristics and high robustness of the system, together with an iso-damping property of the closed loop reference response. The effectiveness of the proposed method is illustrated through the control simulation of three degrees of freedom robot manipulator.

Keywords: robust control, robot manipulator, fractional-order lead/lag compensator, symmetrical optimum, iso-damping property.

1. Introduction

Robotics is a relatively young field of modern technology that crosses traditional engineering boundaries. Understanding the complexity of robots and their applications requires knowledge of electrical, mechanical and systems engineering, computer science and mathematics. The science of robotics has grown tremendously over the past twenty years, fueled by rapid advances in computer and sensor technology, as well as theoretical advances in control theory. At the present time, the vast majority of robot applications deal with industrial robot arms operating in factory environments. Robots are being deployed to accomplish tasks having strict requirements of

accuracy, precision, repeatability, mass production and quality in addition to ease of human effort and cost effectiveness. Typical example applications of robots in industry include welding, packaging, arranging, cutting, paint spraying, moving and sanding. These tasks call for the deployment of manipulator-based robots in industry.

Design of a controller for a manipulator is a complex task. Research community reports few reviews on control strategies for robotic manipulators. A good survey of early results is given by Sage et al. in [1]. Many of these control algorithms follows linear approach from one simple reason. Namely, linear controllers are designed for manipulators whose dynamics are more or less linear (manipulators with high gear ratios, gravity compensation devices, etc.), or have been (partially) linearized by feedback linearization techniques. This way, nonlinearities become less important, dynamic coupling effects from the motion of other joints can be neglected and robot control can be decoupled into independent joint control. That is why classical PID controller has been used as a usual tool for the stabilization of robot manipulators in real applications [2-4].

On the other side, during the last 20 years, efforts have been made to implement the fractional calculus techniques in control theory. The fractional calculus is theory of integrals and derivatives of arbitrary order, i.e. orders other than integer [5]. In most cases, objective is to apply the fractional order control to improve the control system characteristics. Intuitively, with non integer controllers there is higher flexibility in adjusting the system performances than using integer order controllers. Fractional order (FO) controller gives us tool to design robust control system with less parameters to tune. This way, FO controller with few tuning knobs achieves robustness which is similar to using very high order controllers. Also, the tradeoff between system performances and stability is more straightforward to achieve by introducing fractional order control. In the literature, different structures have been introduced for linear, time invariant, fractional order controllers. Some of the most common include CRONE controller [6,7], $PI^\lambda D^\mu$ controller [8], and fractional lead/lag compensator [9-11].

The transient and steady state system response can be improved with (fractional) lead/lag compensator, and by adjusting the system's phase and gain margin. It is well known the phase margin defines the relative stability and influences on the transient response characteristics, while the speed of system response is proportional to the bandwidth of the system. So, by changing the gain crossover frequency one could reshape the system's bandwidth and its speed response. The transfer function of fractional order (FO) lead/lag compensator, which is a generalization of the classical compensator, is given by:

$$C(s) = K_C \left(\frac{as+1}{bs+1} \right)^\alpha, \tag{1}$$

where K_C is the compensator gain, α is the fractional order of the controller $(\alpha > 0)$, $1/a$ is the zero frequency, and $1/b$ is the pole frequency ($a < b$ for a lag compensator). The influence of parameter α is remarkable. With lower value of α the distance between the zero and pole becomes longer and vice versa, and contribution of phase at a certain frequency stands still. Because of this fact the controller is more flexible and allows considerations of robustness in the design. For example, with some control techniques an iso-damping property of the closed loop system can be achieved [7,12]. The fractional order lag compensator is commonly used to improve tracking performance and disturbance attenuation at low frequencies. For $a > b$ we obtain lead compensation which is used to improve phase margin. In this paper, fractional order lag compensator is designed to enhance closed loop performance of robot manipulator.

Most of the methods for tuning linear controllers are based on solving specific optimization problems considering main four sensitivity functions [13]. Besides these, alternative methods

such as symmetrical and non-symmetrical optimum have been developed. A symmetrical optimum method originates from Kessler's work in [14]. Later it was exploited in several papers [15-17], and herein it will be used for tuning the parameters of fractional order lag compensator. The idea behind the symmetrical optimum principle is that phase frequency characteristics $\varphi(\omega)$, i.e. characteristic $\varphi_{pm}(\omega) = 180° + \varphi(\omega)$ of the open-loop transfer function is symmetrical relative to the straight line perpendicularly drawn to the frequency axis in gain crossover frequency (ω_{gc}, 0 dB). The use of this idea is illustrated in Figure 1. By using this fact, it is possible to form symmetrical criterion which may be stated as: several odd-order derivatives of phase characteristic of open-loop function should tend to zero in the gain crossover frequency ω_{gc}. Then, parameters of fractional order compensator can be obtained by solving optimization procedure with respect to symmetrical criterion and specified phase margin [18,19].
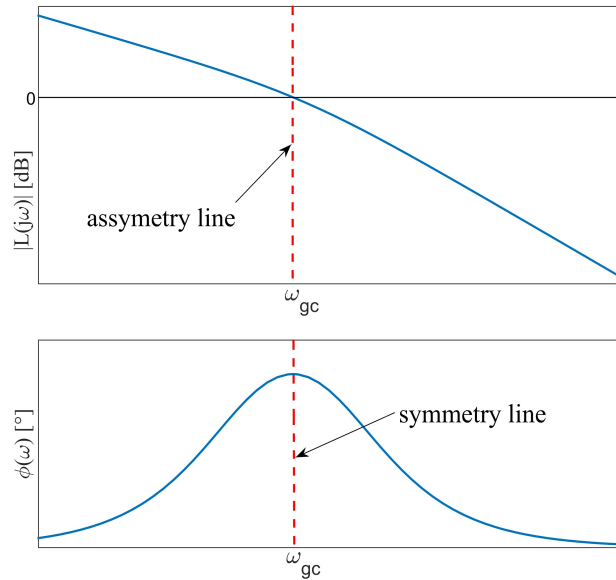

Fig. 1. Illustration of symmetrical optimum principle.

The rest of the paper is organized as follows. In Section 2 mathematical model of robot manipulator with actuator dynamics is derived using the Rodriquez approach. The optimization problem setup for the given model is presented in Section 3, including the symmetrical optimum constraints. The efficiency of the fractional order controller is demonstrated in Section 4 through the simulation of NeuroArm robotic manipulator. Section 5 concludes the paper.

2. Mathematical model of robot manipulator with actuator dynamics

The mechanical structure of a robot manipulator consists of a sequence of rigid bodies (or links) interconnected by means of joints. In this paper Rodriquez approach [20] is used to obtain equations of motion. The open chain system of rigid bodies (V_1), (V_2), … , (V_n) is shown in Figure 2. The rigid body (V_1) is connected to the fixed stand. Two neighboring bodies (V_{i-1}) and (V_i) are connected together with a joint (i), which allows translation or rotation of the body (V_i) in respect to body (V_{i-1}). The values q^i represent generalized coordinates. The reference frame $Oxyz$ is inertial Cartesian frame, and the reference frame $O\xi\eta\zeta$ is local body frame which is associated to the body (V_i). At initial time, the corresponding axes of reference frames were parallel. This configuration is called reference configuration and it is denoted by (0).

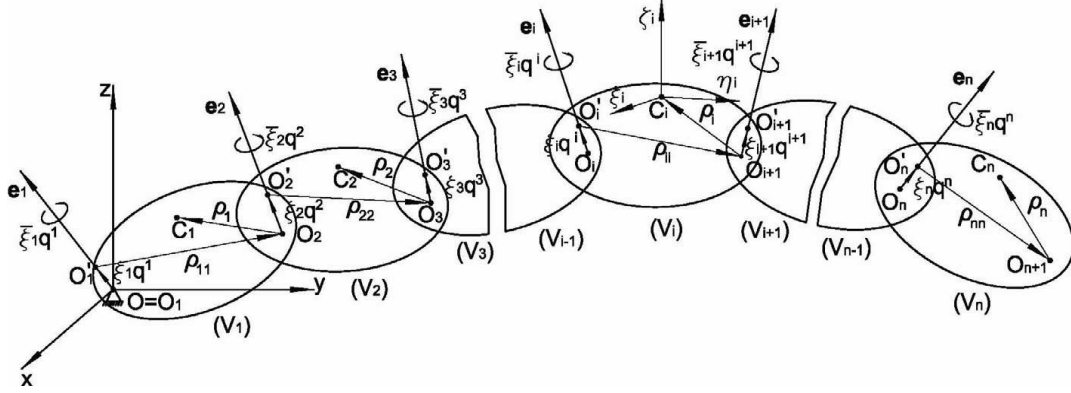Fig. 2. Open chain of the rigid bodies system.

The geometry of the system is defined by the unit vectors $\vec{e}_i$ and position vectors $\vec{\rho}_i$ and $\vec{\rho}_{ii}$ expressed in local coordinate systems $C_i \xi_i \eta_i \zeta_i$ connected to mass centers of bodies in a multibody system. Unit vector $\vec{e}_i$, $i=1,2,\ldots,n$ is describing the axis of rotation (translation) of the i-th segment with respect to the previous segment, and $\vec{\rho}_{ii} = \overrightarrow{O_i' O_{i+1}}$ denotes a vector between two neighboring joints in a multibody system, while position of the center of mass of i-th segment is expressed by vectors $\vec{\rho}_{ii} = \overrightarrow{O_{i+1}' C_i}$. For the entire determination of this mechanical system, it is necessary to specify masses m_i and tensors of inertia J_{Ci} expressed in local coordinate systems.

If we have a kinetic energy of the system in terms of generalized coordinates and its derivatives, one can write dynamic equations of the system in terms of Lagrange equations of the second kind. The motion imposed to a manipulator's joint is realized by an actuating system which usually consists of a DC servomotor and a transmission (gear). After some transformations, equations of motion of a rigid robot together with an actuating system can be written as

$$\left(A(q) + N^2 J_m\right)\ddot{q} + \left(C(q,\dot{q}) + N^2 B_m\right)\dot{q} - Q^g = Q^m, \tag{2}$$

wherein:

n is a number of bodies in the system,

$q(t) \in \mathbb{R}^n$ is the vector of the generalized coordinates,

$A(q) \in \mathbb{R}^{n \times n}$ represents basic metric tensor (or inertia matrix),

$C(q,\dot{q}) \in \mathbb{R}^{n \times n}$ is a matrix that includes centrifugal and Coriolis effects,

$Q^g \in \mathbb{R}^n$ and $Q^m \in \mathbb{R}^n$ are gravity term and torque vectors applied to the joints, respectively,

N is the $n \times n$ diagonal matrix of the gear ratios,

J_m is the $n \times n$ diagonal matrix containing the effective motors inertias, and finally,

B_m is the $n \times n$ diagonal matrix containing the viscous friction coefficients of the motors.

For details of the calculation of the basic metric tensor and matrix $C(q,\dot{q})$ for robot manipulators, the reader is referred to [20]. The torques Q^m are supplied by n actuators. In the case of a rigid robot, the standard equations describing the transmission of the gears are

$$q_m = Nq, \quad Q^m = N\tau_m, \tag{3}$$

wherein q_m represents the positions of the actuators shafts, and τ_m is the vector of torques supplied by the actuators. Combining (2) with (3) yields the following model of the actuators system

$$J_m \ddot{q}_m + B_m \dot{q}_m = \tau_m - \tau_l, \tag{4}$$

wherein $\tau_l = \left(N^2\right)^{-1}\left(A(q)\ddot{q}_m + C(q,\dot{q})\dot{q}_m\right) - N^{-1}Q^g$ is the vector of torques resulting from the robot manipulator and acting on the motors shafts. A block diagram of the resulting model is shown in Figure 3. In this approach, the positions of the actuators shafts are the controlled variables. One advantage of this approach is that the model of actuators used for the design is linear and decoupled. Another advantage is that torque τ_l resulting from the robot links can now be regarded as disturbance. This assumption is justified if actuators with high gear ratios are used (typically N attains values from a few tens to a few hundred). This way, we can neglect completely the nonlinear dynamics of the robot and use linear model instead.
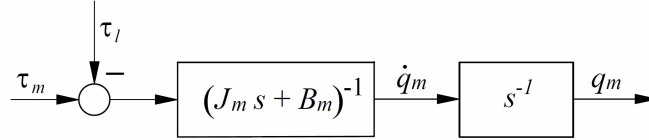

Fig. 3. Block diagram of the DC motors mechanical part.

However, in reality the robot is not controlled by torque signals, but by voltage signals. Consequently, in order to have a more realistic model of the robot, it may be necessary to include the electrical model of the actuators. The complete block diagram with actuator dynamics is shown in Figure 4.
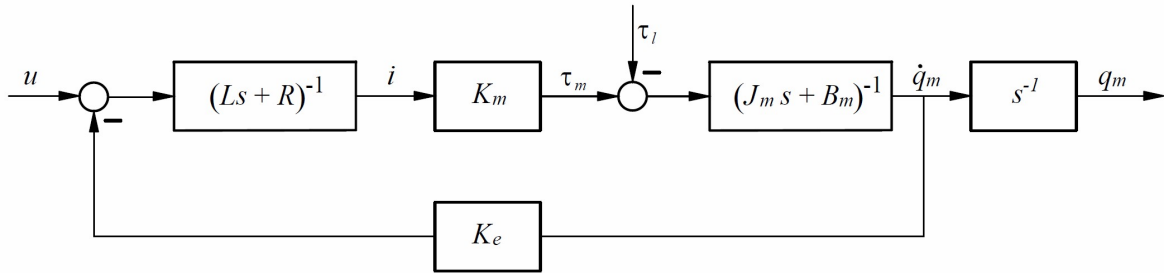

Fig. 4. Block diagram of the DC motors dynamical model.

As it can be seen from the figure, the electrical model of DC actuator is given by

$$R\boldsymbol{i} + L\frac{d\boldsymbol{i}}{dt} + K_e \frac{d\boldsymbol{q}_m}{dt} = \boldsymbol{u}, \tag{5}$$

where R is the $n \times n$ diagonal matrix containing the resistances of the armature circuits, $\boldsymbol{i} \in \mathbb{R}^n$ represents the vector of the armature currents, L is the diagonal matrix of the armature inductances, K_e is the diagonal matrix containing the back EMF constants, and $\boldsymbol{u}$ is the vector of the armature input voltages. The vector of torques supplied by the actuators is

$$\boldsymbol{\tau}_m = K_m \boldsymbol{i}, \tag{6}$$

where K_m is the diagonal matrix containing the motor torque constants. Now, the differential equation describing the motors' mechanical dynamics can be rewritten as Eq. (4).

5

Since the original nonlinear system resulted into n linear, decoupled subsystems, it is enough to observe one arbitrary actuator (joint), and use obtained results for the control system design of other joints. Based on Figure 4, the relationship between the control input u and the position output q_m of the j-th actuator $(1 \le j \le n)$ can be expressed in a unified manner by the transfer function

$$G_p(s) = \frac{k_m}{(\ell s + r)(j_m s + b_m) + k_m k_e} \frac{1}{s} \approx \frac{K}{s(Ts+1)}, \tag{7}$$

where

$$K = \frac{1}{k_e}, \quad T = \frac{j_m r}{k_m k_e}. \tag{8}$$

and $k_m \in K_m$, $k_e \in K_e$, $j_m \in J_m$, $b_m \in B_m$, $\ell \in L$, $r \in R$ and $b_m \approx 0$. The second order transfer function is reduced to a first order model because response of the system is characterized by the dominant pole (the other pole is located far left in the s-plane, and its influence can be neglected). Now, the fractional order lag compensator (1) can be designed for controlling the process $G_p(s)$ given by (7)-(8), and its parameters can be obtained using the symmetrical optimum principle.

3. Symmetrical optimum (SO) design method

The control system scheme with fractional order compensator $C(s)$ is shown in Figure 5 with following notation: $G_p(s)$ - process transfer function, $r(t)$ - reference signal, $y(t)$ - output signal, $u(t)$ - control signal, $d(t)$ - disturbance, $n(t)$ - measurement noise. Reference response signal can be additionally improved through feed-forward filter denoted with $F(s)$.
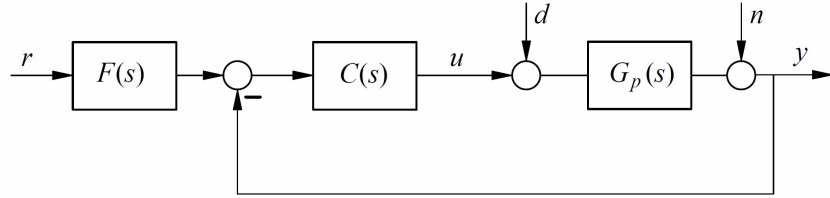

Fig. 5. The proposed control structure with fractional order compensator.

The open loop transfer function of the system in Fig. 5 is given by

$$L_{ok}(s) = C(s)G_p(s). \tag{9}$$

As stated before, the idea behind the symmetrical optimum principle is that phase frequency characteristics $\varphi(\omega)$ of open-loop function is a symmetrical function in $\varepsilon -$ neighborhood of gain crossover frequency ω_{gc}. Symmetrical criterion for function $\varphi(\omega)$ can be expressed in the following form

$$\mu_p = \left. \frac{\partial^p \varphi(\omega)}{\partial \omega^p} \right|_{\omega = \omega_{gc}} = 0, \quad p = 1,3,5,\dots \tag{10}$$

Since relation (10) cannot be valid for all values of integer p, it is suitable to use $p = 1,3$ which will ensure sufficient degree of symmetry of frequency characteristics of L_{ok} around gain

6

crossover frequency ω_{gc}. Another constraint of the closed loop system is desired phase margin defined by

$$\varphi_{\text{pm}}(\omega_{gc}) = 180° + \varphi(\omega_{gc}), \quad \left| L_{\text{ok}}(j\omega_{gc}) \right| = 1. \tag{11}$$

Adjustable parameters of fractional order lag compensator are K_C, a, b and fractional order parameter α. The objective function is given in the form of high-order derivative of phase characteristic of open-loop transfer function. Considering relations (10)-(11), optimization procedure of FO compensator can now be given in the following form

$$\begin{aligned} &\min_{K_C, a, b, \alpha} (\mu_3)^2 \\ &\left| L_{\text{ok}}(j\omega_{gc}) \right| = 1, \\ &180° + \varphi(\omega_{gc}) = \varphi_{\text{pm}}^*, \\ &\mu_1(K_C, a, b, \alpha, \omega_{gc}) = 0, \end{aligned} \tag{12}$$

and solved by using some of the standard nonlinear optimization methods. Initial values of parameters of FO compensator can be empirically selected. Now, the effectiveness of the proposed design procedure will be tested on a process $G_p(s)$ representing a typical DC motor.

3.1 Application of the SO method for the control design of a DC motor

The DC motor provided for this simulation is RE 36 $(\varnothing 36 \text{ mm})$, brushed, 70 Watt from Maxon motors. The parameters used in the modeling are extracted from the data sheet of this motor. Only the following parameters relevant for the model are used: $j_m = 65.2 \text{ gcm}^2$, $r = 1.71 \, \Omega$, $k_m = 44.5 \text{ mNm}/A$, $k_e = 215 \text{ rpm}/V$. Based on these parameters and (7)-(8), the $G_p(s)$ becomes

$$G_{\text{m}}(s) = \frac{22.515}{s(0.0056409s + 1)}. \tag{13}$$

Considering the next design specifications: steady state error $\varepsilon_{ss} = 0$, gain crossover frequency $\omega_{gc} = 10 \text{ rad/s}$ and phase margin $\varphi_{\text{pm}}^* = 45°$, and applying the optimization procedure given by (12), the following parameters of FO compensator are obtained

$$K_C = 6.6517, \, a = 0.0114243, \, b = 21.7816, \, \alpha = 0.503186. \tag{14}$$

So, the transfer function of optimal fractional order lag compensator is given as

$$C_{\text{opt}}(s) = 6.6517 \left(\frac{0.0114243s + 1}{21.7816s + 1} \right)^{0.503186}. \tag{15}$$

The Bode plots of $C_{\text{opt}}(s)$, $G_{\text{m}}(s)$ and $L_{\text{opt}}(s) = C_{\text{opt}}(s) G_{\text{m}}(s)$ are shown in Figure 6. It is clear that the structure proposed meets the condition of phase and magnitude given by design specifications. Moreover, the fractional compensator $C_{\text{opt}}(s)$ guarantees the robustness of the system. Namely, in a wide range around gain crossover frequency $\omega_{gc} = 10 \text{ rad/s}$ phase plots of

$C_{opt}(s)$ and $L_{opt}(s)$ are nearly flat, and hence the phase margin $\varphi_{pm}(\omega)$ is nearly constant. This behavior ensures maximum stability and robustness for wide variations in the plant gain.
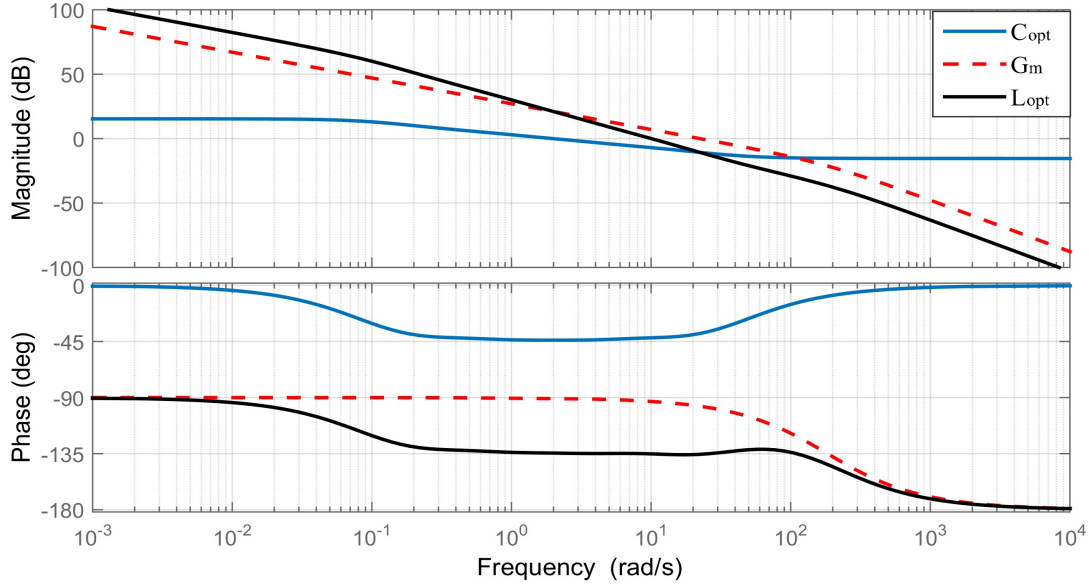

Fig. 6. Bode plots of the compensator $C_{opt}(s)$, process $G_m(s)$ and open-loop transfer function $L_{opt}(s)$.

The same optimization procedure described above can be used for designing control systems of other DC motors actuating robot links.

4. Simulation results

Now, the effectiveness of the proposed control method was examined by computer simulation of a manipulator robot. The manipulator used for simulation is a NeuroArm robotic arm, shown in Figure 7. It is an integral part of the Laboratory of Applied Mechanics, at Faculty of Mechanical Engineering in Belgrade.
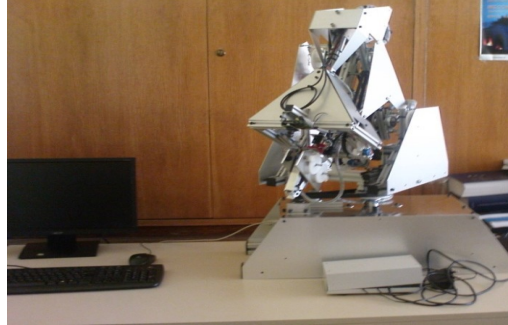

Fig. 7. Laboratory NeuroArm robotic manipulator.

This arm has seven degrees of freedom. First three revolute joints are used for positioning of the end-effector, and the following three joints form the spherical wrist used to accomplish end-effector's orientation. The last joint is the gripper. Since the goal of this paper is designing a controller for positioning tasks, we will simplify our robotic arm to three degrees of freedom (DOF) model considering only the first three joints.

The robot links are actuated by the same type of the DC motor whose transfer function is given with (13). Hence, all three FO compensators will have the same parameter values which

will give optimal controller in the form of (15). Since $C_{\mathrm{opt}}(s)$ is an irrational transfer function, it is difficult to implement this fractional order element in the time domain simulations. Thus, it is necessary to approximate FO compensator with a rational transfer function in the s-domain. Herein, we considered a simple rational representation for fractional order compensators of the form (1) using Padé approximation [21]. The Padé approximation is widely used in numerical calculations of non-rational functions because it provides better approximations compared to some other available methods. So, the fourth order Padé approximation of the transfer function (15) of fractional order compensator is given by

$$C_{\mathrm{pade}}(s) = \frac{0.16926(s+37.27)(s+5.673)(s+1.434)(s+0.3108)}{(s+12.88)(s+2.79)(s+0.7055)(s+0.1076)}. \tag{16}$$

The mechanical coupling between the servomotor and actuated joint is realized by a pair of spur gears. The gear reduction ratio for each of the first three links is $N_{\mathrm{r}} = 230$. As mentioned before, the presence of a high reduction ratio tends to linearize the system, allowing the nonlinear coupling terms in the dynamic model to be neglected.
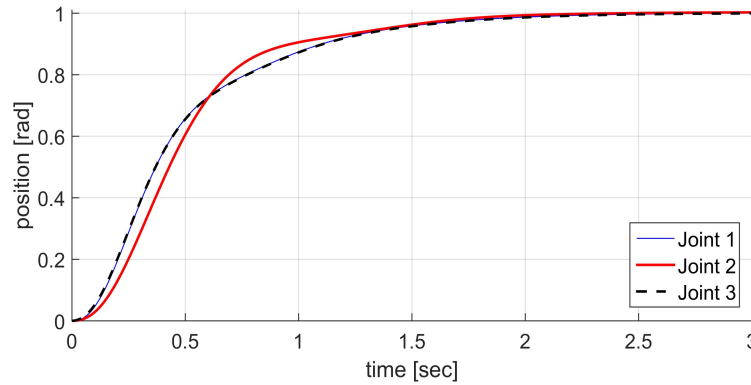

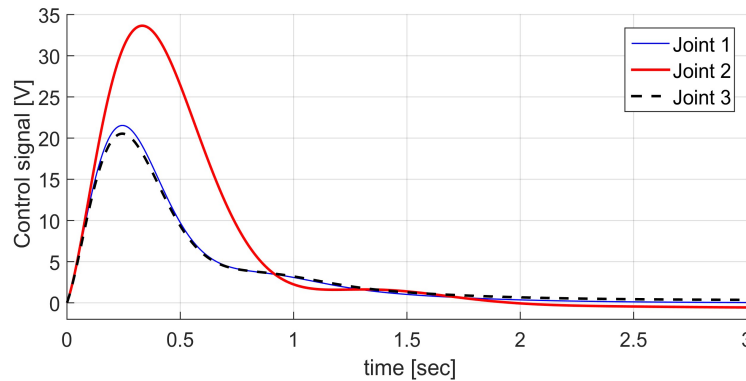Fig. 8. Reference step responses of the three DOFs robot manipulator.

Fig. 9. Control signals for the three DOFs robot manipulator.

Since the controller $C_{\mathrm{opt}}(s)$ (and its approximation (16)) gives constant, but large overshoot of 30%, in order to reduce it, we introduced feed-forward filtering of the command signal in the form $F(s) = 1/(0.5s+1)$. Now, using compensator approximation (16) in simulation, we obtained reference step responses of first three joints which are depicted in Figure 8, and their corresponding control signals are shown in Figure 9. As we can see, the simulated step responses show no overshoot. Having in mind flatness of the phase curve (in Fig. 6) around ω_{gc}, this

behavior is guaranteed for wide variations in the process gain. Hence, the fractional order lag compensator consolidates a good dynamic performance with an improved robustness.

5. Conclusions

This paper deals with the design of the fractional order lag compensator. Parameter values of fractional controller are obtained in optimization procedure by using the symmetrical optimum principle. Thanks to the parameter α, the fractional order of the controller, it has been proved that the lag region for the fractional structure is much wider than for the conventional one. Because of this fact the controller is more flexible and allows considerations of robustness in the design. A robust closed loop response with no overshoot is obtained in a control simulation of three degrees of freedom robot manipulator.

Acknowledgement

References

[1] H.G. Sage, M.F. De Mathelin, E. Ostertag, *Robust control of robot manipulators: A survey*, Inter J Control, vol.76, no.16, pp. 1498-1522, 1999.
[2] G.K. McMillan, *Industrial applications of PID control*. In: Vilanova R, Visioli A, eds. PID control in the third millenium. London: Springer, pp. 415-461, 2012.
[3] T.B. Šekara, M.R. Mataušek, *Optimization of PID Controller Based on Maximization of the Proportional Gain Under Constraints on Robustness and Sensitivity to Measurement Noise*, IEEE Trans Automat Contr, vol. 54, pp. 184-189, 2009.
[4] M.R. Mataušek, T.B. Šekara, *PID controller frequency-domain tuning for stable, integrating and unstable processes, including dead-time*, J Process Control, vol. 21, pp. 17-27, 2011.
[5] S.G. Samko, A.A. Kilbas, O.I. Marichev, *Fractional Integrals and Derivatives: Theory and Applications*. Gordon and Breach, 1993.
[6] A. Oustaloup, B. Mathieu, P. Lanusse, *The CRONE control of resonant plants: application to a flexible transmission*, European Journal of Control, vol. 1, no. 2, 1995. -12.
[7] A. Oustaloup, X. Moreau, M. Nouillant, *The CRONE suspension*, Control Eng. Practice, vol. 4, no.8, pp.1101-1108, 1996.
[8] I. Podlubny, *Fractional-order systems and $PI^\lambda D^\mu$-controllers*, IEEE Trans.Autom.Cont, vol.44, pp.208–214, 1999.
[9] C.A. Monje, Y.Q. Chen, B.M. Vinagre, D. Hue, V. Feliu, *Fractional-order Systems and Control: Fundamentals and Applications*, Springer-Verlag, London, 2010.
[10] M.S. Tavazoei, M.Tavakoli-Kahki, *Compensation by fractional-order phase-lead/lag compensators*, IET Control Theory Applications, vol.8. pp. 319-329, 2014.
[11] M. Safaei, S. Tavakoli, *Tuning of robust fractional-order phase-lead compensators using pole placement and pole-zero ratio minimization*, Journal of Vibration and Control, pp.1-12, January 2018.
[12] H.F. Raynaud, A. Zergainoh, *State-space representation for fractional order controllers*, Automatica, vol.36, pp. 1017–1021, 2000.
[13] T.B. Šekara, *Modern methods of design, analysis, optimization and implementation of conventional control algorithms for processes with finite and infinite degrees of freedom*, International Journal of Electrical Engineering and Computing, vol. 1, no. 1, 2017.
[14] C. Kessler, *Das symmetrische optimum*, Regelungstechnik 6, pp. 395-400 and 432–436, 1958.
[15] K.J. Åström, T. Hägglund, *PID Controllers Theory Design and Tuning*, 2nd ed., ISA, 1995.
[16] J.W. Umland, M. Safiuddin, *Magnitude and Symmetric Optimum Criterion for the Design of Linear Control Systems*, IEEE Trans. Ind. App., vol. 26, No. 3, pp. 489-497, 1990.
[17] G. Maione, P. Lino, *New tuning rules for fractional PI^α controllers*, Nonlinear Dyn., vol. 49, pp. 251-257, 2007.
[18] T.B. Šekara, G.Vuković, B.Blanuša, M.R.Rapaić, B.Jakovljević, *A novel method for optimization of PI/PID regulators base on symmetrical optimum method*, Proc. Infoteh-Jahorina Conf., pp.804-807, 2015 (in Serbian).
[19] M.Č.Bošković, M.R.Rapaić, T.B.Šekara, V.Govedarica, *Non-symmetrical Optimum Design Method of fractional order PID controller*, Proc. INDEL Conf., pp.1-5, 2018.
[20] V. Čović, M. P. Lazarević, *Robot Mechanics*, Faculty of Mechanical Engineering, Belgrade, Serbia, 2009.
[21] M.Č.Bošković, M.R.Rapaić, T.B.Šekara, P.D.Mandić, M.P.Lazarević, B.Cvetković, B.Lutovac, M.Daković, *On the rational representation of Fractional Order Lead Compensator using Pade Approximation*, Proc. 7th MECO Conference, pp.1-4, 2018.